

# Climate and topography control the size and flux of sediment produced on steep mountain slopes

Clifford S. Riebe<sup>a,1</sup>, Leonard S. Sklar<sup>b</sup>, Claire E. Lukens<sup>a</sup>, and David L. Shuster<sup>c,d</sup>

<sup>a</sup>Department of Geology and Geophysics, University of Wyoming, Laramie, WY 82071; <sup>b</sup>Department of Earth and Climate Sciences, San Francisco State University, San Francisco, CA 94132; <sup>c</sup>Department of Earth and Planetary Science, University of California, Berkeley, CA 94720; and <sup>d</sup>Berkeley Geochronology Center, Berkeley, CA 94709

Edited by Thomas Dunne, University of California, Santa Barbara, CA, and approved September 1, 2015 (received for review February 22, 2015)

**Weathering on mountain slopes converts rock to sediment that erodes into channels and thus provides streams with tools for incision into bedrock. Both the size and flux of sediment from slopes can influence channel incision, making sediment production and erosion central to the interplay of climate and tectonics in landscape evolution. Although erosion rates are commonly measured using cosmogenic nuclides, there has been no complementary way to quantify how sediment size varies across slopes where the sediment is produced. Here we show how this limitation can be overcome using a combination of apatite helium ages and cosmogenic nuclides measured in multiple sizes of stream sediment. We applied the approach to a catchment underlain by granodiorite bedrock on the eastern flanks of the High Sierra, in California. Our results show that higher-elevation slopes, which are steeper, colder, and less vegetated, are producing coarser sediment that erodes faster into the channel network. This suggests that both the size and flux of sediment from slopes to channels are governed by altitudinal variations in climate, vegetation, and topography across the catchment. By quantifying spatial variations in the sizes of sediment produced by weathering, this analysis enables new understanding of sediment supply in feedbacks between climate, tectonics, and mountain landscape evolution.**

weathering | erosion | critical zone | detrital thermochronometry

The interplay of climate and life drives weathering on mountain slopes (1–4), converting intact bedrock into mobile sediment particles ranging in size from clay to boulders (5, 6). Water, wind, and biota sweep these particles across slopes under the force of gravity and erode them into channels, where they serve as tools that cut into underlying bedrock during transport downstream (7). Both the size and flux of particles eroded from slopes into channels can influence incision into bedrock (8, 9), which in turn governs the pace of erosion from slopes where the sediment is produced (10, 11). The relationships between sediment production, hillslope erosion, and channel incision imply that they are central to feedbacks that drive mountain landscape evolution (12). When channel incision and hillslope erosion are relatively fast, sediment particles spend less time exposed to weathering on slopes (13) and thus may be coarser when they enter the channel (14), promoting faster incision into bedrock (7). Integrated over time, channel incision and hillslope erosion generate topography (15), imposing altitudinal gradients in precipitation, temperature, and hillslope form (16), and thus ultimately influencing erosion (17), weathering (1), and the sizes of sediment produced on slopes (2). Thus, the size and erosional flux of sediment may both depend on and regulate rates of channel incision into bedrock via feedbacks spanning a range of scales and processes.

Feedbacks between climate, erosion, and tectonics have been widely studied (8, 16, 18–23). However, understanding the role of sediment size remains a fundamental challenge (6–9, 12), due to a lack of methods for quantifying how the size distributions of sediment particles vary across the slopes where sediment is produced from bedrock by weathering and erosion (5, 6). Here we show how to overcome this limitation using a combination of

tracing methods on multiple sediment sizes collected from streams in steep landscapes. Results from the Sierra Nevada, California, enable new understanding of connections between climate, mountain topography, and sediment supply.

## Tracking Multiple Sediment Sizes in a Steep Catchment

Our approach exploits two widely used sediment tracing tools: detrital thermochronometry, which identifies the elevations of hillslopes where sediment was produced by weathering of underlying bedrock (24–27), and cosmogenic nuclides in stream sediment, which reflect the erosion rate of the sediment averaged over the hillslopes where particles in the sample were produced (28). Thus, whereas detrital thermochronometry can be used to quantify spatial variations in sediment production, cosmogenic nuclides in detrital minerals can be used to quantify spatially averaged erosion rates of sediment contributing areas.

Detrital thermochronometry is well illustrated at Inyo Creek, which drains the eastern flanks of the High Sierra (Fig. 1 and *SI Appendix*, Fig. S1). Across catchment slopes, apatite helium ages in bedrock increase with elevation (24), from ~20 My near the catchment mouth to ~70 My at the summit of Lone Pine Peak (Fig. 1, *SI Appendix*, and *Dataset S1*). Thus, sediment collected from the creek should have apatite helium ages that reveal the relative contributions of different elevations to the sediment flux at the sampling point (24). In the reference case of uniform sediment production and erosion, each point on the landscape is equally prone to producing a sediment particle and delivering it to the creek (29, 30). In that case, the measured age distribution

## Significance

Rivers carve through landscapes using sediment produced on hillslopes by biological, chemical, and physical weathering of underlying bedrock. Both the size and supply rate of sediment influence the pace of river incision and landscape evolution, but the connections remain poorly understood, because the size distributions of sediment supplied from slopes have been difficult to quantify. This study combined existing sediment-tracing techniques in a previously unidentified approach to quantify sediment production across an alpine catchment in the High Sierra, California. Results show that colder, steeper, and less vegetated slopes produce coarser sediment that erodes faster into the channel network. These results demonstrate that the sediment-tracing approach can be used to quantify feedbacks between climate, topography, and erosion.

Author contributions: C.S.R., L.S.S., C.E.L., and D.L.S. designed research; C.S.R., L.S.S., C.E.L., and D.L.S. performed research; C.S.R., L.S.S., C.E.L., and D.L.S. contributed new reagents/analytic tools; C.S.R., L.S.S., C.E.L., and D.L.S. analyzed data; and C.S.R., L.S.S., and C.E.L. wrote the paper.

The authors declare no conflict of interest.

This article is a PNAS Direct Submission.

Freely available online through the PNAS open access option.

<sup>1</sup>To whom correspondence should be addressed. Email: [criebe@uwyo.edu](mailto:criebe@uwyo.edu).

This article contains supporting information online at [www.pnas.org/lookup/suppl/doi:10.1073/pnas.1503567112/-DCSupplemental](http://www.pnas.org/lookup/suppl/doi:10.1073/pnas.1503567112/-DCSupplemental).

in creek bed sediment should be similar in shape to the age distribution in underlying bedrock (24–27, 29, 30), calculated by combining the catchment’s elevation distribution with its age–elevation relationship (Fig. 1). Thus, any inconsistencies between the age distributions of sediment and bedrock delimit elevations that differ from the reference case of spatially uniform sediment production and delivery to the creek.

Cosmogenic nuclides serve as tracers of erosion because they accumulate in minerals in the uppermost few meters of rock and soil during exhumation to the landscape surface. Thus, the concentration of cosmogenic nuclides in eroded sediment reflects the erosion rate of the sediment. Slower erosion yields higher nuclide concentrations, because minerals spend more time near the surface interacting with cosmic radiation. Mixtures of minerals from areas with different erosion rates should reflect the spatially averaged erosion rate of the combined area, because each point on the landscape sheds minerals and thus nuclides in proportion to its erosion rate. Thus, minerals in sediment delivered to a creek should have an average nuclide concentration that reflects the average erosion rate of the sediment contributing area (28).

Although it has not been previously recognized in the literature, erosion rate information from cosmogenic nuclides in multiple sediment sizes can be combined with sediment source information from detrital thermochronometry to quantify altitudinal variations in both the erosion rate and the size distribution of sediment particles across a catchment. As a proof of concept, we used data from two sediment sizes sampled from Inyo Creek at a point where the contributing area spans roughly 2 km of relief (Fig. 1). Climate and topography vary substantially with altitude across the catchment, allowing us to test mechanistic hypotheses about chemical, physical, and biological factors that influence sediment production. From the lowest elevation at the catchment outlet to the highest at Lone Pine Peak, mean annual temperature decreases by nearly 12 °C, average precipitation increases by a factor of ~3, the prevalence of steep slopes increases markedly, and desert scrub and conifers give way to barren alpine slopes (Fig. 1). Thus, higher elevations are colder, steeper, and less vegetated than lower elevations. Meanwhile, the catchment has never been glaciated (24) and has three similar stocks of granodiorite bedrock (Dataset S2), thus minimizing the potentially confounding effects of glacial erosion and differences in lithology (31) in our study of climatic and topographic effects on sediment size and erosion rate.

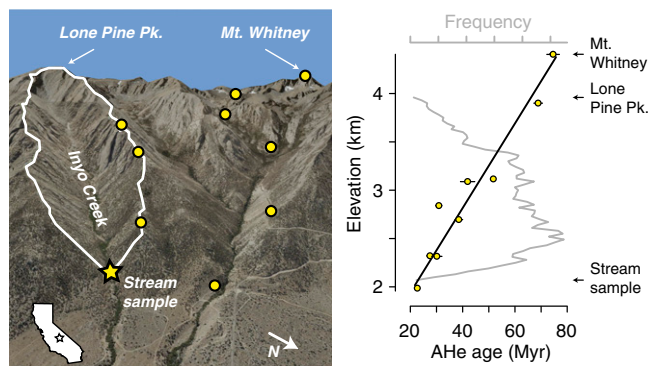


**Fig. 1.** Study site. (Left) Oblique view showing bedrock age locations (circles; after ref. 24), stream sediment sampling site (star), and catchment boundary. (Right) The relative frequency of elevation (gray line; top axis) from a 10-m DEM of the catchment plotted against elevation along with means ( $\pm$  SEM) of apatite helium (AHe) ages (circles; lower axis) for bedrock sampled from locations on Left. Line through data (Right) is least-squares, error-weighted regression of age against elevation.

The differences in climate, topography, and biota across the study catchment should drive altitudinal differences in chemical, biological, and physical weathering (1, 2, 4), which may, in turn, prompt spatial variations in both the size and flux of sediment eroded from slopes. We hypothesize that higher elevations are more strongly influenced by physical weathering and thus produce coarser sediment that erodes faster into the creek than lower elevations, where biological and chemical disaggregation of bedrock dominate. To test our hypothesis, we collected very coarse gravel (32–48 mm diameter) from Inyo Creek (Dataset S3) and measured apatite helium ages and cosmogenic  $^{10}\text{Be}$  in minerals separated from the sediment (SI Appendix and Datasets S4 and S5). This enables comparisons with previously measured apatite helium ages and cosmogenic  $^{10}\text{Be}$  (Datasets S5 and S6) from a sample of finer sediment (24).

## Results

**Spatial Variations in Sediment Size.** By a variety of measures, the very coarse gravel has significantly older apatite helium ages than the finer sediment, indicating that it originated from higher in the catchment (Fig. 2 and SI Appendix, Fig. S2). Both a  $t$  test and a Mann–Whitney  $U$  test demonstrate that the gravel’s apatite is older than finer sediment’s apatite ( $P = 0.0004$  and  $P = 0.00003$ , respectively). Statistically significant differences also emerge from Kolmogorov–Smirnov and Kuiper tests of the measured cumulative age distributions ( $P = 0.0004$  and  $P = 0.0023$ , respectively; SI Appendix and Dataset S7). In addition, Hodges–Lehmann estimators show that paired differences in ages between the gravel and finer sediment have a statistically significant median of 6.3 My and a 95% confidence interval for differences in inferred source elevations of 149–404 m (median = 266 m). These differences are too large to be explained by any differences in the analytical procedures and sampling locations between this study and previous work (SI Appendix).

To explain the measured altitudinal differences in ages in terms of factors that might influence sediment production, we needed to first delimit the elevation ranges that exhibit exceedingly high and low production of gravel and finer sediment. Our benchmark for comparison was the range of plausible measured age distributions in our creek bed samples under the reference condition that each point on the landscape is equally likely to contribute clasts to the creek. We generated plausible distributions for this reference case of uniform erosion using standard bootstrapping methods—i.e., by randomly sampling the bedrock elevation distribution 73 and 52 times, to simulate measured age distributions of gravel and finer sediment, respectively. Each sampled elevation was assigned an age using the age–elevation relationship (Fig. 1), and results were collapsed into an age distribution for each simulation of spatially uniform sediment production and erosion (SI Appendix). Next, we repeated the simulations 30,000 times each and ranked the measured age distributions relative to the simulations at each elevation. Exceptionally low or high percentile ranks, below 2.5 or above 97.5, imply that the measured difference from the median of simulations is unlikely to have arisen by chance when all points on the landscape are contributing equally to sediment in the creek (Fig. 3 A and B). Thus, we identified elevations over which we can be 95% confident that the contributions of the different sizes of sediment are high or low compared with a random sample reflecting uniform sediment production and erosion across the catchment.

Our analysis indicates that the gravel is markedly underrepresented in the 2- to 2.35-km elevation band and overrepresented in the 2.6- to 2.75-km elevation band (Fig. 3A) relative to the case of uniform erosion. The difference is especially pronounced in the lower band: Although it accounts for ~15% of the catchment area, it produced just ~1% of the gravel we sampled from the creek (Fig. 2). Meanwhile, finer sediment is markedly overrepresented in the 2.45- to 2.55-km elevation band and underrepresented in the 3.1- to 3.5-km elevation band relative to

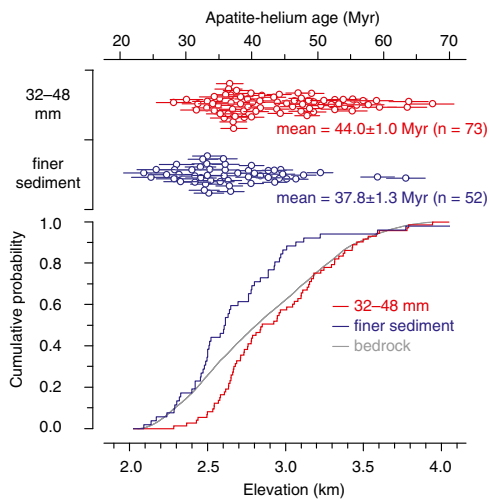


**Fig. 2.** Measured apatite helium ages and inferred erosional source elevations of sediment. (Top) Apatite helium ages ( $\pm$  propagated analytical error) and inferred source elevations for very coarse gravel with diameters of 32–48 mm (red circles) and finer sediment (blue circles; after ref. 24). Means ( $\pm$  SEM) are labeled along with  $n$ , the number of measurements. (Bottom) Cumulative age distributions (CADs, after ref. 25) for very coarse gravel (red line) and finer sediment (blue line). Gray line is CAD for catchment elevations from 10-m DEM ( $n = 33,900$ ). Upper and lower axes are linked by the age–elevation relationship in Fig. 1.

the median of the simulations (Fig. 3B). For example, the upper 30% of the catchment produced just 10% of the sampled finer sediment (Fig. 2). Thus, our results suggest that production of the finer sediment is enhanced at lower elevations and inhibited at higher elevations (Fig. 3B). Overall, nearly half of the catchment’s elevation range exhibits positive or negative departures that lie outside the 95% confidence interval of the uniform erosion simulations for either the gravel or finer sediment (Fig. 3). Thus, detrital thermochronometry reveals sharp contrasts in the erosional source elevations of the two sediment samples.

**Spatial Variations in Erosion Rates.** Measurements of cosmogenic nuclides reveal similarly sharp differences in the rates at which the different sizes of sediment have been shed from the slopes where they are produced to the sampling point in the channel. The cosmogenic  $^{10}\text{Be}$  concentrations in quartz from the gravel and finer sediment are  $1.01(\pm 0.05) \times 10^5$  and  $1.56(\pm 0.01) \times 10^5$  atoms per gram, respectively (SI Appendix and Dataset S5). These results imply two markedly different spatially averaged erosion rates for the catchment, according to conventional methods for interpreting detrital  $^{10}\text{Be}$  data (28). The discrepancy arises because the two sediment sizes represent erosion from different elevations of the catchment in different proportions (Fig. 2). Thus, the  $^{10}\text{Be}$  results from Inyo Creek reveal a complication in interpreting cosmogenic nuclide data from sediment in steep landscapes: When eroded sediment size is spatially variable, any one size class of sediment considered in isolation can yield a distorted perspective on catchment-wide erosion rates. The discrepancies between the age distributions of the gravel and finer sediment (Fig. 2) show that similar errors can arise in studies of detrital thermochronometry (see also ref. 25).

We avoided some of the potential for misinterpretation of sediment tracing data by integrating the erosion rate information with the information on the sizes of sediment produced at different elevations. The  $^{10}\text{Be}$  data show that hillslopes are eroding faster at elevations where the coarser sediment is dominantly produced. Meanwhile the apatite helium ages clearly show that the coarser sediment was eroded from higher elevations, on average, than the

finer sediment (Fig. 2). Thus, we can interpret the  $^{10}\text{Be}$  and apatite helium data together to indicate that erosion rates increase with elevation across the catchment. To quantify this relationship more precisely, we used an optimization algorithm to search for the altitudinal gradient in erosion rates that best matches the measured

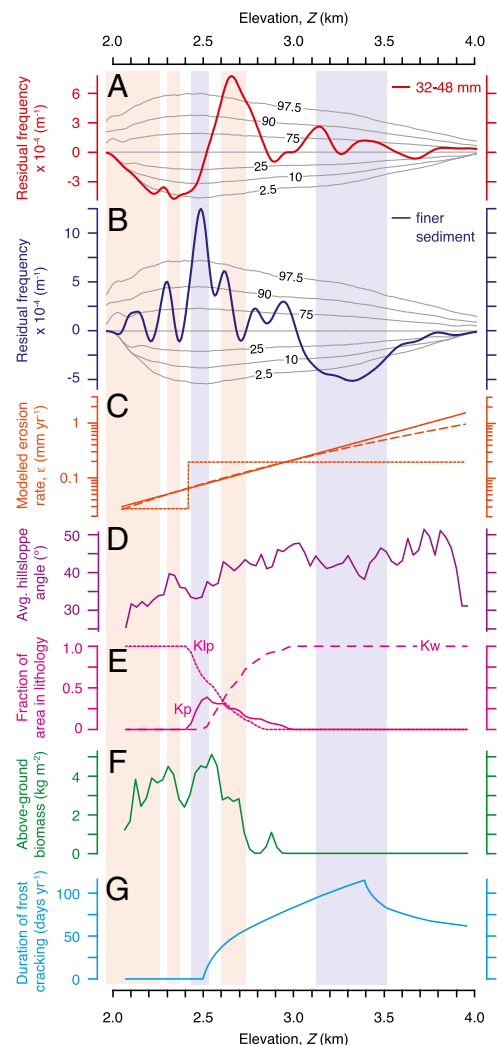


**Fig. 3.** Altitudinal variations in sediment production and driving factors (Dataset S8). Apatite helium ages of very coarse gravel (A) and finer sediment (B) expressed as differences between measured age distributions (see SI Appendix, Fig. S1) and median of 30,000 simulations of uniform erosion from the catchment. Labeled gray lines (A and B) show percentiles of departures from median for all simulations. Light blue and red vertical bands mark elevations over which measured age distributions (red and blue lines) lie outside the 95% confidence interval of the simulations. (C) Variations in erosion rate ( $\varepsilon$ , in millimeters per year) with elevation ( $Z$ , in kilometers) based on optimization of apatite helium and  $^{10}\text{Be}$  data in very coarse gravel and finer sediment (see SI Appendix). Lines show best fits for exponential (solid:  $\varepsilon = 0.2e^{2.1(Z-Z^*)}$ , where  $Z^* = 2.96$  km, a reference elevation), power-law [dashed:  $\varepsilon = 0.2(Z/Z^*)^{5.5}$ ], and step-wise (dotted) functions. Best-fit linear function implies negative erosion for slopes near catchment mouth (an impossible scenario). Average hillslope angle (D) from 10-m DEM increases with elevation ( $r^2 = 0.39$ ,  $P < 0.0001$ ). (E) Fraction of landscape area at each elevation underlain by Lone Pine (Klp), Paradise (Kp), and Whitney (Kw) granodiorite. Biomass (F) is resampled at 10-m resolution from a 30-m remotely sensed dataset. (G) Number of days per year in frost-cracking window (with air temperature between  $-3$  °C and  $-8$  °C) inferred from modern temperature data (SI Appendix). Data in D and F were averaged in 30-m elevation bands.

$^{10}\text{Be}$  concentrations. The approach employs a forward model that expresses the catchment as a collection of points with elevations extracted from a 10-m digital elevation model (DEM). The apatite helium ages allow us to specify the elevation distribution of sediment production for gravel and finer sediment (Fig. 2). We considered four functions for the altitudinal increase in erosion rates: linear, exponential, power, and step. The linear, exponential, and power functions each have two adjustable parameters (a slope and an intercept), and the step function has three (a higher value, a lower value, and an elevation where it changes). For each function, we adjusted the parameters incrementally, ran a forward model of sediment erosion for every parameter combination, and calculated a misfit for each model run as the sum of squared differences between predicted and observed  $^{10}\text{Be}$  concentrations in the sediment (see *SI Appendix*). The parameter combination with the lowest misfit for each function was used to plot erosion rates versus elevation in Fig. 3C. The minimum misfits of the three functions are all similarly low. Moreover, without additional constraints from other sediment sizes, we cannot reliably identify which function agrees best with our observations. Nevertheless, the three best-fit functions in Fig. 3C exhibit a common pattern: Erosion rates increase markedly with altitude. For example, the exponential function shows a fiftyfold increase from  $\sim 0.03 \text{ mm}\cdot\text{y}^{-1}$  at the bottom of the catchment to  $1.5 \text{ mm}\cdot\text{y}^{-1}$  at the top.

## Discussion

Our analysis of detrital thermochronometry and cosmogenic nuclides reveals that both the size and flux of sediment vary markedly across Inyo Creek slopes. The altitudinal increases in sediment size and erosion rates indicate that the catchment harbors considerable spatial variations in effectiveness of processes that break bedrock down and deliver it to channels. These variations likely arise due to altitudinal differences in topography and climate across the catchment.

**Topography, Erosion Rates, and Sediment Size.** Average hillslope angle increases with altitude across most of the catchment (Fig. 3D). Thus, the inferred altitudinal variations in erosion rates correlate strongly with topography for both the exponential and power-law functions (Fig. 4). These trends, together with the broad scatter in erosion rates at steep hillslope angles, match patterns observed in so-called threshold landscapes in previous studies of spatially averaged erosion rates from multiple catchments (17, 32, 33). Here they emerge from a single catchment, illustrating the power of using information from multiple sizes and multiple sediment tracing techniques to quantify spatial variations in the size and flux of sediment produced on slopes.

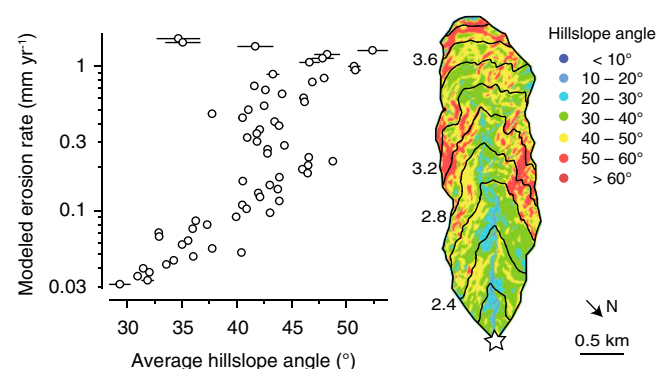


**Fig. 4.** Topographic control of erosion rates. (Left) Erosion rates from best-fit exponential function (Fig. 3C) increase with average hillslope angle. Erosion rates from best-fit power law (see *Dataset S8*) follow a similar, but less steep trend. (Right) Map showing distribution of hillslope angles from the 10-m DEM. Contour interval, 0.2 km. Star, sediment sampling site.

Erosional processes are evidently wearing away slopes in catchment headwaters much faster than slopes near the outlet (Fig. 3C). However, the trends quantified here reflect just a snapshot averaged over the  $10^3$ - to  $10^4$ -y timescales of the methods. Extrapolated over the last several million years, the inferred spatial variations in erosion rates imply substantial headward erosion of the catchment into the low-relief surface of the High Sierra (Fig. 1). In that case, the steepest slopes associated with the fastest erosion rates and coarsest sizes could have reached the modern catchment divide at Lone Pine Peak in just 2–4 My (*SI Appendix*), similar to the time elapsed since movement on the Sierra Nevada Frontal Fault accelerated base-level lowering of streams draining the range (34). This raises the possibility that the catchment itself (Fig. 1) and the altitudinal trends in sediment size and flux (Fig. 3) are all outcomes of a wave of differential erosion that has been propagating into the range since the Pliocene.

Connections between our results and the tectonics of the range are speculative, due to mismatches in timescale. However, the connections between topography and erosion rates are strong (Fig. 4). They are also consistent with our hypothesis about altitudinal controls on weathering and erosion. Moreover, they may help explain the altitudinal distribution of excesses and deficits in production of gravel and finer sediment across the catchment (Fig. 3A and B). Topography and erosion rates can regulate sediment size by influencing sediment residence times, with slower erosion on gentler slopes leading to longer exposure to weathering (3, 35) and thus finer sediment supplied to channels. This hypothesis is consistent with the observed slower erosion and enhanced delivery of the finer sediment from lower, more gently sloped elevations at Inyo Creek (Fig. 3B and C).

**Bedrock and Sediment Size.** Although the mineralogy and geochemistry of the catchment's three mapped bedrock units are similar enough to fall into the same "granodiorite" category, we cannot rule out the possibility that some of the variations in sediment production are due to altitudinal differences in lithology (Fig. 3E and *Dataset S2*). However, all three units have abundant biotite (ref. 36 and *SI Appendix*), which is widely thought to drive granular disintegration in granitic bedrock (37). Moreover, the highest and lowest units, which dominate the catchment (Fig. 3E), are similar in mineral size distribution (*SI Appendix*, Fig. S3) even though the highest unit contains  $\sim 10\%$  K-feldspar megacrysts and the lowest unit contains none (ref. 36 and *Dataset S2*). The abundant biotite and similarities in mineral size across the catchment may help explain why outcrops of the different bedrock units are similarly prone to rapid granular disintegration on slopes where climate is roughly the same (*SI Appendix*, Fig. S3). Thus, we can be reasonably certain that the deficit in fine sediment production at 3.1–3.5 km (Fig. 3B) is not entirely due to an intrinsically lower weathering susceptibility in the highest bedrock unit. Likewise, the fact that the lowest bedrock unit breaks down into a wide range of sediment sizes, both on slopes and in the channel (*SI Appendix*, Fig. S4), indicates that the deficit in gravel production at 2–2.35 km (Fig. 3A) is not entirely due to an intrinsically higher weathering susceptibility in underlying bedrock at low elevations. Thus, we deduce that altitudinal differences in lithology are too small to fully explain the differences in erosion and weathering implied by the sediment tracing data. This may not be the case in other, more geologically diverse catchments; rock type can influence both ecosystems (31) and erosion rates (31, 38), and different lithologies can have differences in bedding, jointing, and tectonic deformation in the crust (39). These factors could contribute to intrinsic differences in the sizes of sediment produced on slopes but do not appear to differ enough to drive the observed patterns in sediment production at Inyo Creek.

**Climate, Erosion Rates, and Sediment Size.** In contrast, differences in climate across the catchment are large and may play a significant role in the altitudinal distribution of excesses and deficits in the production of gravel and finer sediment (Fig. 5). For example, the excess in gravel production from 2.6 km to 2.8 km (Fig. 3A) corresponds to a decrease in biomass and an increase in the duration of frost cracking with elevation (Fig. 3F and G). Slightly higher up, over the band of deficits in finer sediment from 3.1 km to 3.5 km (Fig. 3B), slopes are steep (Fig. 3D), erosion is fast (Fig. 3C), biomass is negligible (Fig. 3F), and the duration of frost cracking is long (Fig. 3G). Physical weathering likely dominates over biological and chemical weathering across these elevations, enhancing production of coarse sediment and limiting production of fine sediment (Fig. 5). Meanwhile, both the deficit in gravel (Fig. 3A) and excess in fine sediment (Fig. 3B) span elevations with relatively gentle slopes (Fig. 3D), slow erosion rates (Fig. 3C), high biomass (Fig. 3F), and negligible frost cracking (Fig. 3G); chemical and biological weathering likely dominate over physical weathering processes, thus favoring production of fine sediment and inhibiting survival of coarse particles (Fig. 5), consistent with the observed distributions of apatite helium ages.

**Chemical, Biological, and Physical Weathering.** The connections shown in Figs. 3–5 are strong, but do not necessarily reflect causation. Nevertheless, they are consistent with the hypothesis that weathering shifts from dominantly biological and chemical near the catchment mouth to dominantly physical in the headwaters, due to altitudinal contrasts in climate and topography. At low elevations, biological and chemical weathering are intense enough, or erosion is slow enough, and soil residence times are commensurately long enough, that coarse rock fragments readily break down to sand and fine gravel before they reach the channel (Fig. 5). Meanwhile, at higher elevations, where physical weathering processes such as frost cracking and rockfall dominate, bedrock shatters into coarser fragments that are delivered rapidly to channels across steep slopes without much additional breakdown (Fig. 5C).

Our analysis of just two size classes yields a much richer understanding of sediment supply than one could obtain from either technique alone applied to a single sediment size. Additional data should reveal whether sediment originates from events spanning

only the elevations represented by the gravel and finer sediment. If such spatially discrete sediment delivery (e.g., by landsliding) were responsible for the patterns in Fig. 2, it would undermine our analysis of spatial variations in erosion rates (Figs. 3C and 4) but not our interpretations of altitudinal variations in sediment size (Figs. 3A–B and 5).

Apatite ages and cosmogenic nuclides from all size classes in the creek should provide a more comprehensive understanding of how size distributions and erosion rates of sediment vary with elevation across catchment slopes. This should aid in deconvolving the effects of climate, vegetation, erosion, topography, and lithology on sediment production. Optimization algorithms similar to those used here will be vital to inferring altitudinal trends in sediment production that are internally consistent with all of the measured geochemical data. With enough data, it should be possible to account for nonuniform distributions of bedrock apatite (27), deep landsliding (40, 41), wildfires (42), nonmonotonic relationships between age and elevation (25, 43), and other complications not present at Inyo Creek. For example, it will be important to solve for size reduction during transport in catchments where sediment is weak or travel distances are long (6, 44). At Inyo Creek, source bedrock is hard, travel distances are short, and we assume that size reduction during transport is negligible. This assumption is conservative, relative to our conclusions about altitudinal increases in sediment size, because size reduction would be greater for the coarser particles that travel farther from higher elevations.

Our approach integrates over the timescales of sediment production and removal, which is less than  $10^4$  y due to fast erosion at Inyo Creek. For a longer-term perspective, our approach could be applied to the archive of sediment in the debris fan at the catchment mouth (Fig. 1) to quantify how climate change has influenced sediment production over time. We expect the effects to be significant, based on the strong climatic control on modern sediment production documented here (Fig. 5).

## Conclusions

Our study provides a framework for quantifying the climatic and geomorphic controls on the sizes of sediment produced on slopes and delivered to channels. Climate and topography both appear to be important in the trends in sediment size across our study site. The observed altitudinal variations in sediment size and flux

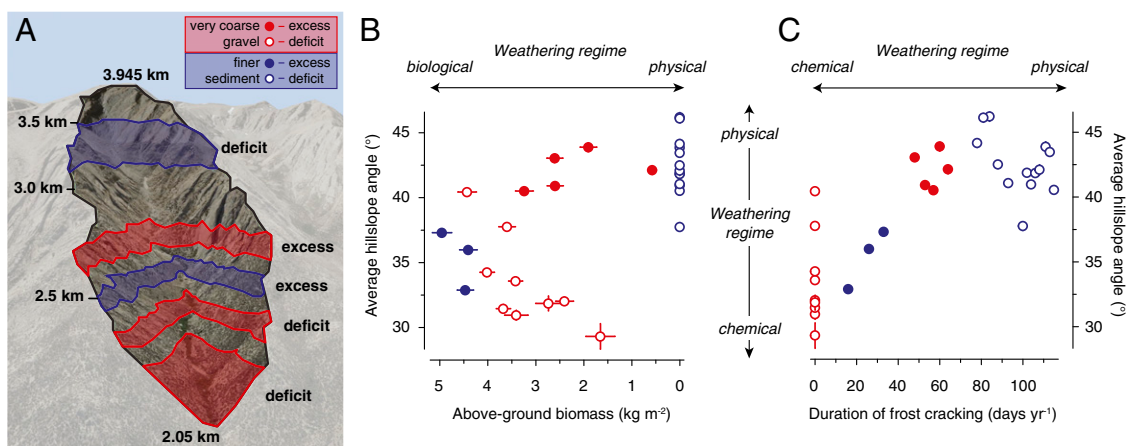


**Fig. 5.** Climatic and topographic control of the sizes of sediment produced on slopes. (A) Oblique view of catchment. Shading marks elevation bands from Fig. 3 of excesses and deficits in production of gravel (red) and finer sediment (blue) relative to the 95% confidence limits on simulated erosion. Plots of hillslope angle against biomass (B) and duration of frost cracking (C) mark conditions with deficits (open circles) and excesses (filled circles). Excesses in gravel and deficits in finer sediment cluster at elevations where physical weathering may be promoted by steep slopes, low biomass, and long durations of frost cracking. Deficits in gravel and excesses in finer sediment tend to cluster at elevations where chemical and biological weathering may be promoted by gentle slopes, high biomass, and short durations of frost cracking.

are robust, but it is difficult to differentiate climatic, topographic, and lithologic effects without data from more sizes. Hence, we cannot readily predict how sediment production varies with altitude in other catchments that harbor different relationships between altitude, slope, climate, and lithology. However, a more predictive understanding will be obtainable if the approach described here is applied across diverse climatic, lithologic, and tectonic settings. Thus, future applications of the approach will contribute to new process-based understanding of hillslope weathering and erosion in steep landscapes. This, in turn, will permit more mechanistic understanding of grain size variations in channel networks (9, 44) and thus reveal how geology, climate, and topography influence riverine habitats (45). Moreover, as shown here, our approach can improve understanding of the role of sediment supply in the feedbacks between climate, erosion, and tectonics that drive landscape evolution across sites where the origins of sediment can be traced. At Inyo Creek, we found rare empirical support for the hypothesis that the

sizes of eroded sediment are coupled to climate and topography through their effects on hillslope erosion, weathering, and sediment production.

## Methods

We used standard techniques to isolate quartz and apatite from samples of sand and gravel collected from the active streambed in 2011. To quantify (U–Th)/He ages of apatite, we sent handpicked crystals to California Institute of Technology for analysis of  $^4\text{He}$ , U, Th, and Sm by noble gas mass spectrometry and inductively coupled plasma mass spectrometry. To quantify  $^{10}\text{Be}$  concentrations, we dissolved quartz, spiked it with  $^9\text{Be}$ , and extracted the Be for analysis of  $^{10}\text{Be}/^9\text{Be}$  ratios by accelerator mass spectrometry at Purdue University.

**ACKNOWLEDGMENTS.** We thank W. J. Hahm for field assistance, X. Ding for laboratory assistance, and J. W. Kirchner for discussions. Funding was provided by the Ann and Gordon Getty Foundation, an American Geophysical Union Horton Research Grant (to C.E.L.), the Doris and David Dawdy Fund for Hydrologic Research, and National Science Foundation Grants EAR 1239521 and 1325033.

- Riebe CS, Kirchner JW, Finkel RC (2004) Sharp decrease in long-term chemical weathering rates along an altitudinal transect. *Earth Planet Sci Lett* 218(3–4):421–434.
- Hales TC, Roering JJ (2005) Climate-controlled variations in scree production, Southern Alps, New Zealand. *Geology* 33(9):701–704.
- Norton K, von Blanckenburg F (2010) Silicate weathering of soil-mantled slopes in an active Alpine landscape. *Geochim Cosmochim Acta* 74(18):5243–5258.
- Brantley SL, et al. (2011) Twelve testable hypotheses on the geobiology of weathering. *Geobiology* 9(2):140–165.
- Marshall JA, Sklar LS (2012) Mining soil databases for landscape-scale patterns in the abundance and size distribution of hillslope rock fragments. *Earth Surf Processes Landforms* 37(3):287–300.
- Attal M, Lavé J (2006) Changes of bedload characteristics along the Marsyandi River (central Nepal): Implications for understanding hillslope sediment supply, sediment load evolution along fluvial networks, and denudation in active orogenic belts. *Spec Pap Geol Soc Am*, 398, pp 143–171.
- Sklar LS, Dietrich WE (2001) Sediment and rock strength controls on river incision into bedrock. *Geology* 29(12):1087–1090.
- Whipple KX (2004) Bedrock rivers and the geomorphology of active orogens. *Annu Rev Earth Planet Sci* 32:151–185.
- Cowie PA, et al. (2008) New constraints on sediment-flux-dependent river incision: Implications for extracting tectonic signals from river profiles. *Geology* 36(7):535–538.
- Wobus C, Heimsath A, Whipple K, Hodges K (2005) Active out-of-sequence thrust faulting in the central Nepalese Himalaya. *Nature* 434(7036):1008–1011.
- Hilley GE, Arrowsmith JR (2008) Geomorphic response to uplift along the Dragon's Back pressure ridge, Carrizo Plain. *Calif Geol* 36(5):367–370.
- Egholm DL, Knudsen MF, Sandiford M (2013) Lifespan of mountain ranges scaled by feedbacks between landsliding and erosion by rivers. *Nature* 498(7455):475–478.
- Mudd SM, Yoo K (2010) Reservoir theory for studying the geochemical evolution of soils. *J Geophys Res* 115(F3):F03030.
- Attal M, et al. (2015) Impact of change in erosion rate and landscape steepness on hillslope and fluvial sediments grain size in the Feather River Basin (Sierra Nevada, California). *Earth Surf Dyn* 3(1):201–222.
- Whipple KX, Tucker GE (1999) Dynamics of the stream-power river incision model: Implications for height limits of mountain ranges, landscape response timescales, and research needs. *J Geophys Res* 104(B8):17661–17674.
- Reiners PW, Ehlers TA, Mitchell SG, Montgomery DR (2003) Coupled spatial variations in precipitation and long-term erosion rates across the Washington Cascades. *Nature* 426(6967):645–647.
- Montgomery DR, Brandon MT (2002) Topographic controls on erosion rates in tectonically active mountain ranges. *Earth Planet Sci Lett* 201(3–4):481–489.
- Ferrier KL, Huppert KL, Perron JT (2013) Climatic control of bedrock river incision. *Nature* 496(7444):206–209.
- Willett SD (1999) Orogeny and orography: The effects of erosion on the structure of mountain belts. *J Geophys Res* 104(B12):28957–28981.
- Montgomery DR, Balco G, Willett SD (2001) Climate, tectonics, and the morphology of the Andes. *Geology* 29(7):579–582.
- Burbank DW, et al. (2003) Decoupling of erosion and precipitation in the Himalayas. *Nature* 426(6967):652–655.
- Whipple KX (2009) The influence of climate on the tectonic evolution of mountain belts. *Nat Geosci* 2(2):97–104.
- Armitage JJ, Duller RA, Whittaker AC, Allen PA (2011) Transformation of tectonic and climatic signals from source to sedimentary archive. *Nat Geosci* 4(4):231–235.
- Stock GM, Ehlers TA, Farley KA (2006) Where does sediment come from? Quantifying catchment erosion with detrital apatite (U–Th)/He thermochronometry. *Geology* 34(9):725–728.
- Vermeesch P (2007) Quantitative geomorphology of the White Mountains (California) using detrital apatite fission track thermochronology. *J Geophys Res* 112(F3):F03004.
- McPhillips D, Brandon MT (2010) Using tracer thermochronology to measure modern relief change in the Sierra Nevada, California. *Earth Planet Sci Lett* 296(3–4):373–383.
- Tranel LM, Spotila JA, Kowalewski MJ, Waller CM (2011) Spatial variation of erosion in a small, glaciated basin in the Teton Range, Wyoming, based on detrital apatite (U–Th)/He thermochronology. *Basin Res* 23(5):571–590.
- Granger DE, Riebe CS (2014) *Treatise on Geochemistry*, ed Drever JE (Elsevier, Oxford), 2nd Ed, pp 401–436.
- Brewer ID, Burbank DW, Hodges K (2003) Modelling detrital cooling-age populations: Insights from two Himalayan catchments. *Basin Res* 15(3):305–320.
- Ruhl KW, Hodges K (2005) The use of detrital mineral cooling ages to evaluate steady state assumptions in active orogens: An example from the central Nepalese Himalaya. *Tectonics* 24(4):TC4015.
- Hahm WJ, Riebe CS, Lukens CE, Araki S (2014) Bedrock composition regulates mountain ecosystems and landscape evolution. *Proc Natl Acad Sci USA* 111(9):3338–3343.
- Binnie SA, Phillips WM, Summerfield MA, Fifield LK (2007) Tectonic uplift, threshold hillslopes, and denudation rates in a developing mountain range. *Geology* 35(8):743–746.
- DiBiase RA, Heimsath AM, Whipple KX (2012) Hillslope response to tectonic forcing in threshold landscapes. *Earth Surf Processes Landforms* 37(8):855–865.
- Wakabayashi J (2013) Paleochannels, stream incision, erosion, topographic evolution, and alternative explanations of paleoaltimetry, Sierra Nevada, California. *Geosphere* 9(2):1–25.
- Ferrier KL, Kirchner JW (2008) Effects of physical erosion on chemical denudation rates: A numerical modeling study of soil-mantled hillslopes. *Earth Planet Sci Lett* 272(3–4):591–599.
- Hirt WH (2007) Petrology of the Mount Whitney Intrusive Suite, eastern Sierra Nevada, California: Implications for the emplacement and differentiation of composite felsic intrusions. *Geol Soc Am Bull* 119(9–10):1185–1200.
- Wahrhaftig C (1965) Stepped topography of southern Sierra Nevada, California. *Geol Soc Am Bull* 76(10):1165–1189.
- Hurst MD, Mudd SM, Yoo K, Attal M, Walcott R (2013) Influence of lithology on hillslope morphology and response to tectonic forcing in the northern Sierra Nevada of California. *J Geophys Res* 118(2):832–851.
- Molnar P, Anderson RS, Anderson SP (2007) Tectonics, fracturing of rock, and erosion. *J Geophys Res* 112(F3):F03014.
- Niemi NA, Oskin M, Burbank DW, Heimsath AM, Gabet EJ (2005) Effects of bedrock landslides on cosmogenically determined erosion rates. *Earth Planet Sci Lett* 237(3–4):480–498.
- Reinhardt LJ, et al. (2007) Interpreting erosion rates from cosmogenic radionuclide concentrations measured in rapidly eroding terrain. *Earth Surf Processes Landforms* 32(3):390–406.
- Reiners PW, Thomson SN, McPhillips D, Donelick RA, Roering JJ (2007) Wildfire thermochronology and the fate and transport of apatite in hillslope and fluvial environments. *J Geophys Res* 112(F4):F04001.
- Stockli DF, Dumitru TA, McWilliams MO, Farley KA (2003) Cenozoic tectonic evolution of the White Mountains, California and Nevada. *Geol Soc Am Bull* 115(7):788–816.
- Sklar LS, Dietrich WE, Fofoulea-Georgiou E, Lashermes B, Bellugi DG (2006) Do gravel bed river size distributions record channel network structure? *Water Resour Res* 42(6):W06D18.
- Riebe CS, Sklar LS, Overstreet BT, Wooster JK (2014) Optimal reproduction in salmon spawning substrates linked to grain size and fish length. *Water Resour Res* 50(2):898–918.